





Numerical analysis of the penetration process of a 30mm armor-piercing projectile

Predrag R. Pantović^a, Miroslav M. Živković^b,
Vladimir P. Milovanović^c, Nenad M. Miloradović^d

^a University of Kragujevac, Faculty of Engineering,
Kragujevac, Republic of Serbia,
e-mail: predragpantovic92@gmail.com, **corresponding author**,
ORCID iD:  <https://orcid.org/0000-0001-6811-7238>

^b University of Kragujevac, Faculty of Engineering,
Kragujevac, Republic of Serbia,
e-mail: miroslav.zivkovic@kg.ac.rs,
ORCID iD:  <https://orcid.org/0000-0002-0752-6289>

^c University of Kragujevac, Faculty of Engineering,
Kragujevac, Republic of Serbia,
e-mail: vladicka@kg.ac.rs,
ORCID iD:  <https://orcid.org/0000-0003-3071-4728>

^d Ministry of Defense of the Republic of Serbia,
Belgrade, Republic of Serbia,
e-mail: nenad.miloradovic@mod.gov.rs,
ORCID iD:  <https://orcid.org/0009-0006-4123-2627>

DOI: 10.5937/vojtehg71-43502; <https://doi.org/10.5937/vojtehg71-43502>

FIELD: mechanical engineering, materials

ARTICLE TYPE: original scientific paper

Abstract:

Introduction/purpose: Thin plates made of high-strength steel are frequently used both in civil and military ballistic protection systems. In order to choose an appropriate type of alloy, it is necessary to fulfil a number of criteria, such as the condition of use, the desired ballistic performance, weight, dimensions, and price. This paper presents a numerical analysis of the penetration of a 30mm armor-piercing projectile with a velocity of 750m/s into steel alloy Weldox 460 plates of different thicknesses at a distance of 1000m .

Methods: The analysis has been performed using numerical methods and finite element modeling to calculate stresses and deformation caused by the penetration effect. For defining material characteristics, the Johnson-Cook material model and the fracture of materials model have been used. In this paper, the software packages FEMAP and LS Dyna have been used for defining models and performing numerical calculations.

Results: The results of the performed numerical analysis as well as the obtained stress and displacement values are presented for four different

armor plate thicknesses: 30mm, 33mm, 34mm, and 40mm. The results show a penetration effect and an interaction between the projectile and the armor plate.

Conclusion: Modeling the impact on armor-piercing obstacles is very complex, extensive, and demanding, and the formed models approximate the real problem of projectile penetration in a very successful way (or with a certain deviation). In recent times, the analysis using the finite element method has proven to be one of effective approaches to solving such and similar problems. The material and the dimensions of the obstacle, as well as the material and the ballistic parameters of the projectile have the greatest influence on projectile penetration. Keeping all the input parameters at the same level and increasing the thickness of the target leads to its increased resistance to penetration.

Keywords: armor, projectile, penetration, Weldox 460, numerical methods.

Introduction

Studying the effect of impact loads and, as a consequence, the resulting damage in a structure, is very demanding and complex. This stems from the very nature of the process, which is a dynamic event, as well as from the problem of defining the resulting damage.

Ballistic penetration is an extremely complex mechanical process that has been researched for more than 200 years. Today, three different directions of research into the problem of penetration can be defined: empirical, analytical, and numerical.

The empirical approach is based on the formation of appropriate relationships between relevant quantities on the basis of experimentally established dependencies. In contrast, analytical methods are characterized by the development of relatively simple models of the penetration process and the application of relevant equations of movement and material behavior, while the numerical approach is characterized by the discretization of the structure into smaller elements and the application of the fundamental laws of physics to each element individually. Each of the three methods for studying penetration has advantages and disadvantages. Numerical analysis has proven to be capable of determining exact solutions for very complex problems, but it is necessary to invest a lot of time for the required calculations. In most cases, it is best to use a combination of all three approaches. Due to the need for computing resources and the costs of performing a large number of parametric studies, there is a considerable interest in transitional solutions or approximate engineering modeling.

Armor-piercing projectiles are intended to destroy armored targets. They penetrate armor thanks to the enormous kinetic energy they have at the moment of collision with an obstacle and the great endurance of their bodies. The importance of the study of penetration is reflected in its application, which has two aspects. The basic field of application is military technique, considering that penetration is one of the most important mechanisms involved in projectile construction, i.e., terminal ballistics.

The consideration of the penetration process is of fundamental importance for the optimization of projectiles with a penetrating effect, as well as for the design of armor protection. On the other hand, there are also numerous civilian applications of the penetration process, such as the protection of facilities (e.g., nuclear power plants), as well as applications in mining and construction.

In this paper, a numerical simulation of the penetration process of a 30mm anti-aircraft armor projectile into plates made of Weldom 460 alloy of different thicknesses have been done. The drawing of the projectile design used in this analysis is shown in Figure 1.

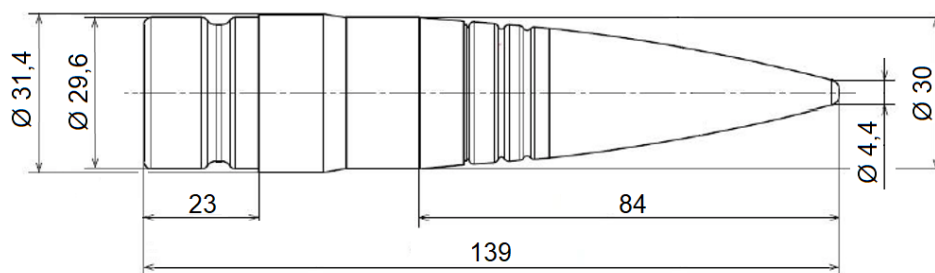


Figure 1 – 30mm projectile, drawing
Рис. 1 – Снаряд 30мм, рисунок
Слика 1 – Пржектил 30 мм, цртеж

The projectile body is made of three different materials:

- Steel *AISI4340* – projectile core,
- Steel *AISI1006* – ballistic cap, and
- Copper – driving ring.

The plate is made of armor steel *Weldom 460*. A 3D model of the projectile design is shown in Figures 2 and 3.

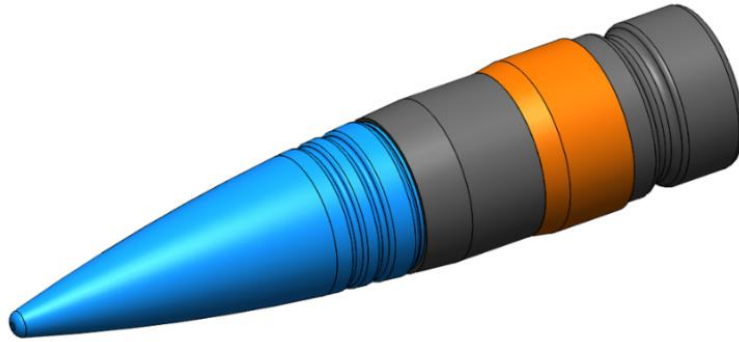


Figure 2 – 30mm projectile, 3D model
 Рис. 2 – Снаряд 30мм, 3Д модель
 Слика 2 – Пројектил 30 мм, модел 3Д



Figure 3 – 30mm projectile parts, 3D model
 Рис. 3 – Части снаряда 30мм, 3Д модель
 Слика 3 – Делови пројектила 30 мм, модел 3Д

The ballistic characteristics of the projectile are presented in Table 1.

Table 1 – Ballistic characteristics of the 30mm projectile
 Таблица 1 – Баллистические характеристики снаряда 30мм
 Табела 1 – Балистичке карактеристике пројектила 30 мм

| | | | |
|---|------------|----------|-----|
| Caliber | d x l | 30 x 165 | mm |
| Projectile weight | m | 0,4 | kg |
| Projectile velocity (at a distance of 0 m) | V_0 | 970 | m/s |
| Projectile velocity (at a distance of 1000 m) | V_{1000} | 750 | m/s |
| Max pressure at 15°C | P_{max} | < 3500 | bar |

Theoretical basis

Penetration process

All bodies filled with explosives or some other substance capable of causing a certain effect on the target are called by a common name – ammunition. Today, a large number of different types of ammunition are in use and are distinguished from each other by purpose, shape, structural parameters, launch method, effect on the target, etc.

This type of projectile is used in cannons from 20mm caliber up to the heaviest ones, that is, in all cannons where it is possible to give the projectile such an initial speed that the trajectory is flat, and the impact speed is such that the kinetic energy of the projectile is sufficient to overcome the resistance of a hard obstacle – body armor.

The armor-piercing projectile penetrates the armor thanks to the kinetic energy it has at the moment of collision with the armor and the great endurance of its body.

Penetration, i.e., breaking through, is the process of movement of the penetrator through an obstacle. Every movable body designed for penetration is called a penetrator, and the target body exposed to the influence of a moving penetrator is called an obstacle. The study of the penetration process is of great importance both in the field of civilian application and in the field of military technology.

Terminal ballistics is one of the basic disciplines that deals with the definition of penetration mechanisms, which significantly contributes to the optimization of the design of projectiles with a penetrating and destructive effect, as well as to the design of armor protection.

On the other hand, there are also numerous civilian applications of the penetration process, such as the protection of buildings, etc. Applications for military purposes are certainly a priority and the most important driver of research in the field of penetration (Elek, 2018).

The basic types of penetration processes characteristic of armor-piercing ammunition are shown in Figure 4.

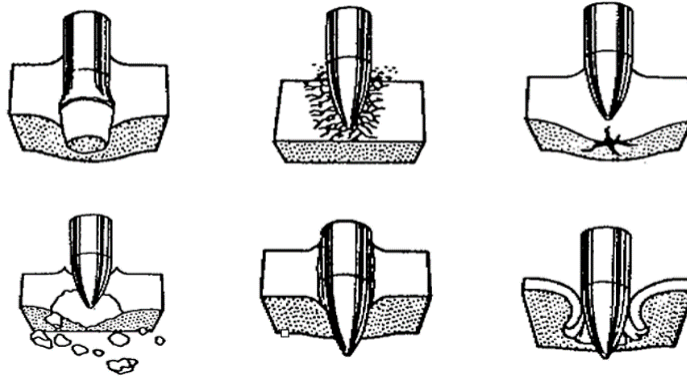


Figure 4 – Basic types of penetration processes
 Рис. 4 – Основные типы процессов проникновения
 Слика 4 – Основни типови пенетрационих процеса

Depending on the outcome of the penetration process, four different cases are distinguished:

- **Penetration** – implies the passage of the entire penetrator through the obstacle, whereby a regular, approximately cylindrical opening is formed in the obstacle,
- **Limited penetration** – represents the borderline case of penetration because the opening in the obstacle is irregularly shaped and has a smaller area than the area of the cross-section of the penetrator, in contrast to a breakthrough, i.e. only parts of the broken penetrator pass through the opening,
- **Semi penetration** – characterized by stopping (jamming) of the penetrator in an obstacle or breaking it during penetration, and
- **Ricochet** – represents the repulsion of the penetrator due to sliding on the surface of the obstacle if it is inclined.

The penetrating power of a penetrator is the ability to break through an obstacle. Increasing penetrating power of the penetrator can be achieved by increasing the length and density of the penetrator, as well as by reducing its diameter. Conversely, the ability to resist penetration represents the resilience of an obstacle. Increasing the resistance of the obstacle is achieved by increasing its thickness and density, as well as by improving the mechanical characteristics of the material (Elek, 2018).

In the last few years, a large number of papers in the field of ballistic penetration have been published. Some of them contain detailed descriptions and give certain recommendations for various engineering models and numerical techniques, and there are also activities on the

development of new models of the penetration process. In addition, great efforts have been made to obtain models and algorithms for simulating the actual response of materials under high-velocity loading. Equations of state and the calculation of strength effects require the definition of constitutive models.

Johnson-Cook material model

Johnson and Cook proposed a semi-experimental constitutive model for metals characterized by high stresses, high strain rates and high temperatures. Each of the phenomena (strain hardening, strain hardening rate and thermal softening) is represented by an independent factor. Taking all factors into account, yield stress is obtained as a function of effective plastic strain, rate of plastic strain and temperature (Wang & Shi, 2013; Liu et al, 2012).

Johnson and Cook represent yield stress by equation 1:

$$\sigma_y = (A + B\bar{\epsilon}_p^n)(1 + c\ln\dot{\epsilon}^*)(1 - T^{*m}) \quad (1)$$

where A is the initial yield stress, B is the reinforcement coefficient, n is the amplification exponent, c is the deformation rate constant and m is the thermal softening exponent.

$\bar{\epsilon}_p$ is the effective plastic deformation and $\dot{\epsilon}^*$ is the effective plastic strain rate for $\dot{\epsilon}_0 = 1s^{-1}$ given by equation 2:

$$\dot{\epsilon}^* = \frac{\bar{\dot{\epsilon}}_p}{\dot{\epsilon}_0} \quad (2)$$

Temperature is given by equation 3:

$$T^* = \frac{T - T_{room}}{T_{melt} - T_{room}} \quad (3)$$

where T_{room} is the room temperature and T_{melt} is the material melting temperature.

The constants for materials are determined by various types of tests, such as tensile test, Hopkinson rod test, etc.

The deformation of the material during damage is given by equation 4:

$$\epsilon^f = [D_1 + D_2 \exp(D_3\sigma^*)](1 + D_4 \ln \epsilon^*)(1 + D_5 T^*) \quad (4)$$

where $D_i, i = 1, \dots, 5$ are the parameters that define the material damage criteria and σ^* is the ratio of the pressure divided by the effective stress.

Material failure occurs when the parameter (equation 5):

$$D = \sum \frac{\bar{\varepsilon}_p}{\varepsilon^f} \quad (5)$$

reaches the value of 1.

Mie-Grüneisen equation of state

The Mie–Grüneisen equation of state represents the relationship between pressure and volume of a solid at a given temperature. It is used to determine the pressure in solids exposed to high pressure for a short period of time. There are several different relations that define a given dependency. Grüneisen's model can be presented in the form given by equation 6 (Heuzé, 2012; Wilkins, 1999):

$$\Gamma_0 = V \left(\frac{dp}{dE} \right)_V \quad (6)$$

where Γ_0 is the Grüneisen parameter which represents the thermal pressure arising from a set of vibrating atoms, V is the volume, p is the pressure and E is the internal energy.

If it is assumed that Γ_0 does not depend on pressure and internal energy, it can be written (equation 7):

$$p - p_0 = \frac{\Gamma_0}{V} (E - E_0) \quad (7)$$

where p_0 is the reference pressure at a temperature $T = 0K$ and E_0 is the reference internal energy at a temperature $T = 0K$.

In that case, p_0 and E_0 are also independent of temperature, so the values of these parameters can be estimated from Hugoniot's equation-equation 8, 9 and 10 (Heuzé, 2012; Wilkins, 1999).

One version of the equation of state is

$$p = \frac{\rho_0 C_0^2 \chi \left(1 - \frac{\Gamma_0}{2} \chi \right)}{(1 - s\chi)^2} + \Gamma_0 E \quad (8)$$

$$\chi = 1 - \frac{\rho_0}{\rho} \quad (9)$$

$$s = \frac{dU_s}{dU_p} \quad (10)$$

where C_0 is the speed of sound through the material, ρ_0 is the initial density of the material, ρ is the current density of the material, Γ_0 is the Grüneisen parameter, s is the linear slope coefficient of Hugoniot's line, U_s is the

shock wave speed, U_p is the particle velocity and E is the internal energy per unit of reference volume.

Material characteristics

The Johnson-Cook's parameters for different types of materials used in the numerical simulation of the penetration of a 30mm armor-piercing projectile are defined in Table 2 and the temperature parameters are given in Table 3. In Table 4, the damage parameters for the same materials are defined. These parameters are defining the Johnson–Cook material model used in numerical simulations (Murthy & Santhanakrishnanan, 2020; Bataev et al, 2019; Champagneet al, 2010; Rezasefatet al, 2018).

Table 2 – Johnson–Cook parameters for different materials
Таблица 2 – Параметры Джонсона–Кука для различных материалов
Табела 2 – Џонсон–Кукови параметри за различите материјале

| Material | A [MPa] | B [MPa] | n | C | M |
|-----------------|---------|---------|------|--------|------|
| Steel AISI 4340 | 792 | 510 | 0.26 | 0.014 | 1.03 |
| Steel AISI 1006 | 350 | 275 | 0.36 | 0.022 | 1 |
| Copper | 90 | 292 | 0.31 | 0.025 | 1.09 |
| Weldox 460 | 490 | 807 | 0.73 | 0.0114 | 0.94 |

Table 3 – Thermal characteristics for different materials
Таблица 3 – Тепловые характеристики различных материалов
Табела 3 – Термичке карактеристике за различите материјале

| Material | T_{melt} [K] | c_p [J/kgK] |
|-----------------|----------------|---------------|
| Steel AISI 4340 | 1793 | 477 |
| Steel AISI 1006 | 1811 | 450 |
| Copper | 1356 | 383 |
| Weldox 460 | 1800 | 452 |

Table 4 – Damage parameters for different materials
Таблица 4 – Параметры повреждения различных материалов
Табела 4 – Параметри оштећења за различите материјале

| Material | D_1 | D_2 | D_3 | D_4 | D_5 |
|-----------------|--------|-------|-------|--------|-------|
| Steel AISI 4340 | 0.05 | 3.44 | –2.12 | 0.002 | 0.61 |
| Steel AISI 1006 | –0.8 | 2.1 | –0.5 | 0.0002 | 0.61 |
| Copper | 0.54 | 4.89 | –3.03 | 0.014 | 1.12 |
| Weldox 460 | 0.0705 | 1.732 | –0.54 | –0.015 | 0 |

Table 5 defines the parameters of the equation of state for different materials used in the numerical simulation.

*Table 5 – Equation of state parameters for different materials
Таблица 5 – Параметры уравнения состояния различных материалов
Табела 5 – Параметри једначине стања за различите материјале*

| Material | C_0 [mm/s] | s | Γ_0 |
|-----------------|--------------------------------|-----------------------|------------------------------|
| Steel AISI 4340 | $3.850 \cdot 10^6$ | 1.354 | 1.707 |
| Steel AISI 1006 | $3.075 \cdot 10^6$ | 1.294 | 1.587 |
| Copper | $3.940 \cdot 10^6$ | 1.489 | 1.990 |
| Weldox 460 | $3.574 \cdot 10^6$ | 1.920 | 1.690 |

Finite element modeling

The creation of the model using the finite element method is performed on the basis of the existing projectile 3D model. Since the analysis system has two symmetry planes (along the projectile axis), a quarter model is created to obtain faster calculation results. In accordance with the shape and construction of the tested projectiles and the plate, in order to properly define the network, a 3D eight-nodes element type hexa is used. The projectile and plate models are shown in Figures 5, 6 and 7. The finite element model of the projectile is modeled using 141000 nodes and 127000 elements, while the 10mm thick plate is modeled using 1275000 nodes and 1200000 elements. The average size of the elements is 0.5mm.

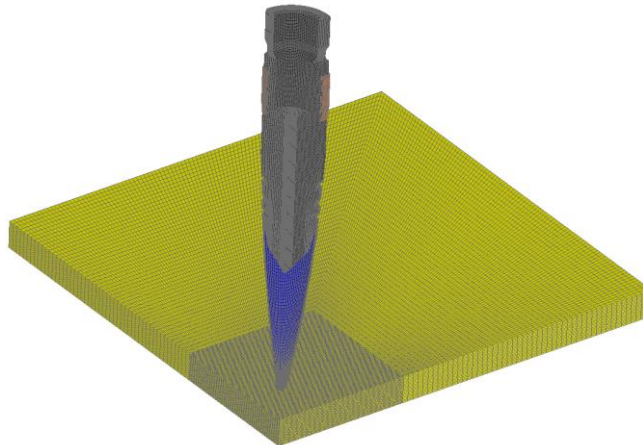


*Figure 5 – FEM model of the projectile and the plate, isometry
Рис. 5 – МКЭ-модель снаряда и пластины, изометрија
Слика 5 – МКЕ модел пројектила и плоче, изометрија*

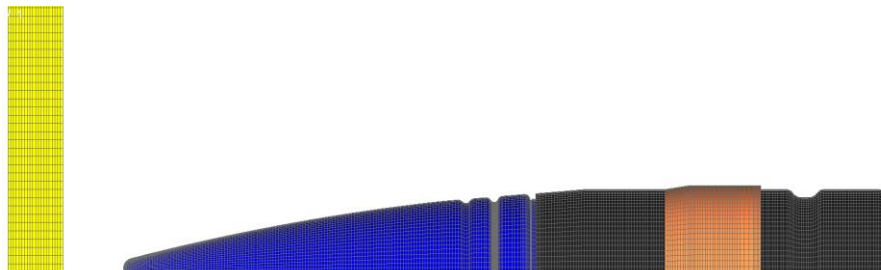


Figure 6 – FEM model of the projectile and the plate, side view
 Рус. 6 – МКЭ-модель снаряда и пластины, вид сбоку
 Слика 6 – МКЕ модел пројектила и плоче, бочни поглед



Figure 7 – FEM model of the projectile elements
 Рус. 7 – МКЭ модель элементов снаряда
 Слика 7 – МКЕ модел елемената пројектила

After creating the projectile model and the plate model, the initial and boundary conditions are defined.

Numerical simulation of the penetration process is performed for the value of the projectile impact speed of 750m/s. The reason for choosing this velocity value is that, for 30mm armor-piercing ammunition, penetration is defined at a distance of 1000m from the mouth of the cannon barrel, and the defined velocity of the projectile is a table value at that distance.

Results and discussion

In this chapter, the results for four different cases are presented. Every case represents one plate thickness: 30mm, 40mm and two additional cases for determining the projectile maximum penetration: 33mm and 34mm.

By increasing the thickness of the armor plate, probability that the projectile will have full or partial penetration decreases, and vice versa.

In each case, the constant parameter is the projectile velocity and it has a value of 750m/s.

Case 1 – Plate thickness of 30mm

Figures 8-13 show the Von Misses equivalent stress and penetration effect for armor plate Weldox 460 with a thickness of 30mm.

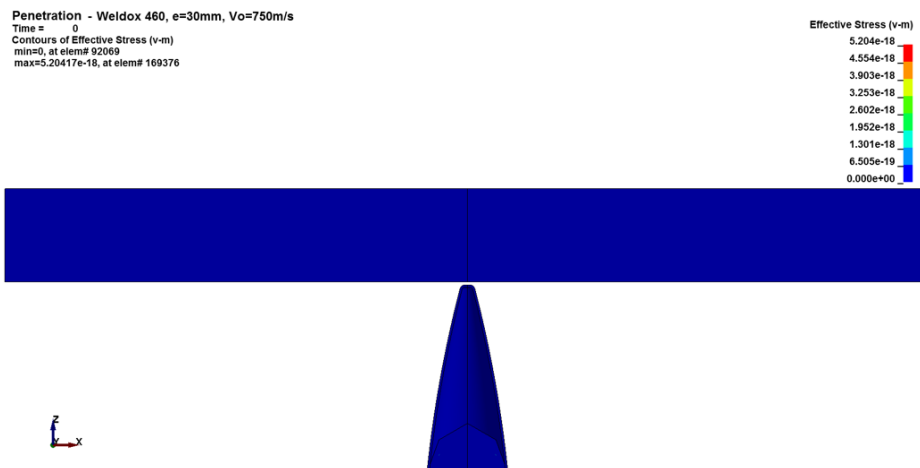


Figure 8 – Von Misses equivalent stress, step 1 – case 1
 Рис. 8 – Эквивалентное напряжение Фон Мизиса, шаг 1 – случай 1
 Слика 8 – Вон Мисесов еквивалентни напон, корак 1 – случај 1

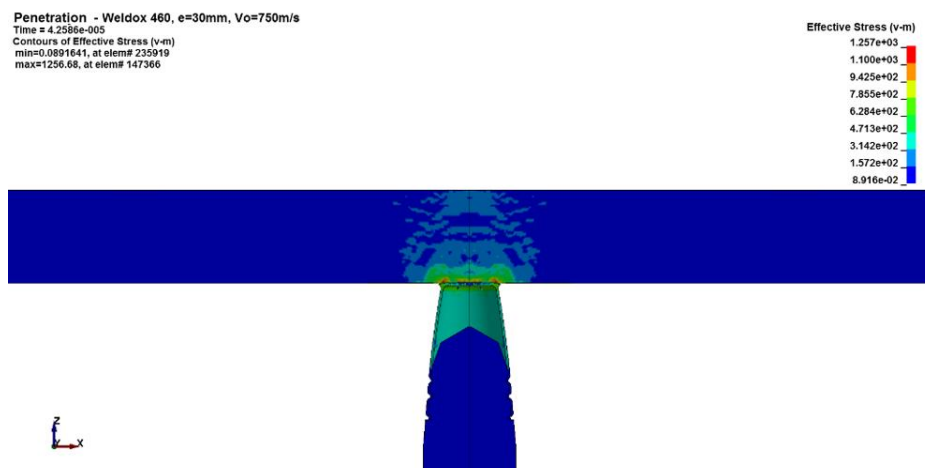


Figure 9 – Von Misses equivalent stress, step 2 – case 1
 Рис. 9 – Эквивалентное напряжение Фон Мизиса, шаг 2 – случай 1
 Слика 9 – Вон Мисесов еквивалентни напон, корак 2 – случај 1

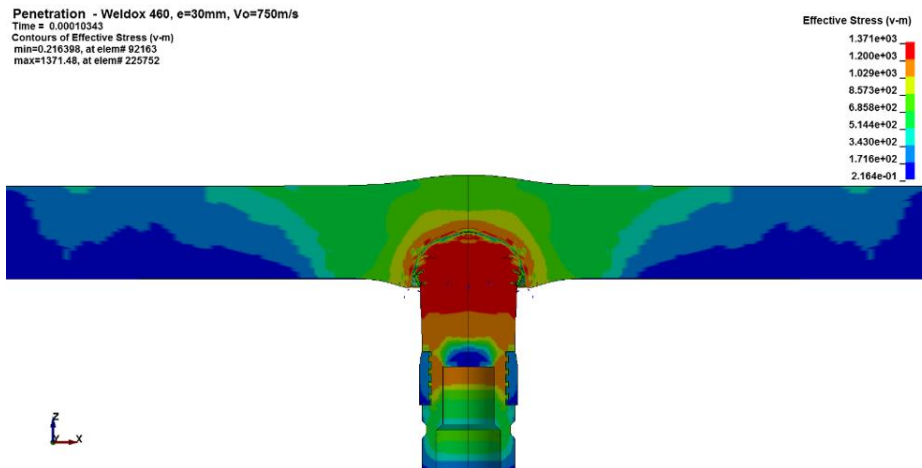


Figure 10 – Von Misses equivalent stress, step 3 – case 1
 Рис. 10 – Эквивалентное напряжение Фон Мизиса, шаг 3 – случай 1
 Слика 10 – Вон Мисесов еквивалентни напон, корак 3 – случај 1

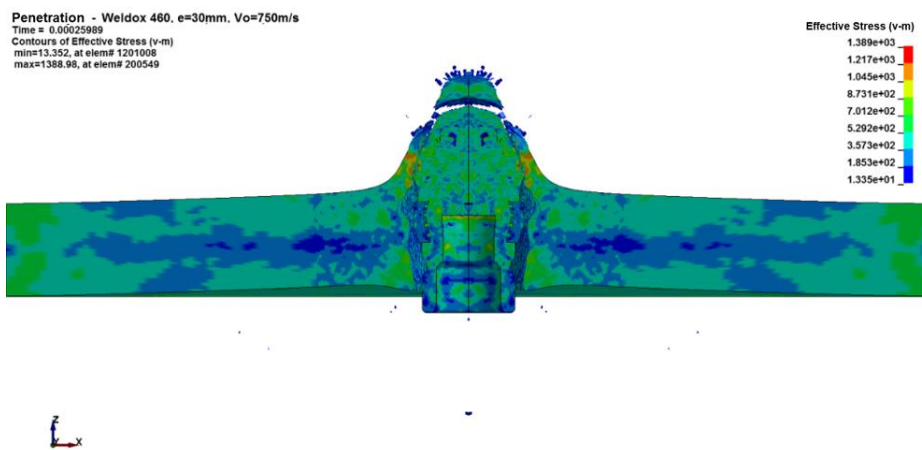


Figure 11 – Von Misses equivalent stress, step 4 – case 1
 Рис. 11 – Эквивалентное напряжение Фон Мизиса, шаг 4 – случай 1
 Слика 11 – Вон Мисесов еквивалентни напон, корак 4 – случај 1

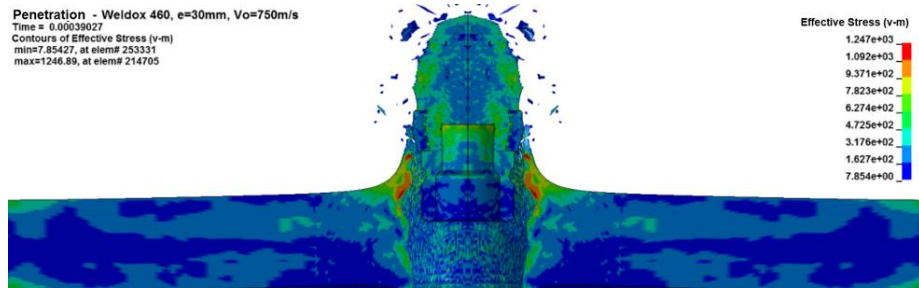


Figure 12 – Von Mises equivalent stress, step 5 – case 1
 Рис. 12 – Эквивалентное напряжение Фон Мизиса, шаг 5 – случай 1
 Слика 12 – Вон Мисесов еквивалентни напон, корак 5 – случај 1

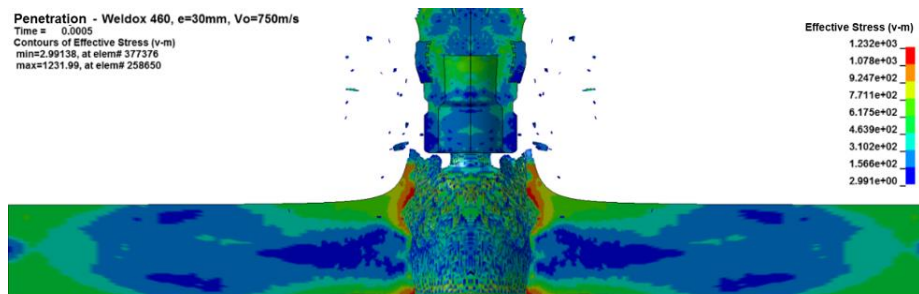


Figure 13 – Von Mises equivalent stress, step 6 – case 1
 Рис. 13 – Эквивалентное напряжение Фон Мизиса, шаг 6 – случай 1
 Слика 13 – Вон Мисесов еквивалентни напон, корак 6 – случај 1

As the results from Figures 8-13 show, the projectile has sufficient kinetic energy to achieve a full penetration effect in the plate of a thickness of 30mm. A large number of fragments are created behind the armor plate as separated parts of both the projectile and the plate.

Figure 14 shows the projectile velocity from the moment when it starts penetration into the plate until the moment of passing through the plate. The projectile velocity after penetration is 220m/s.

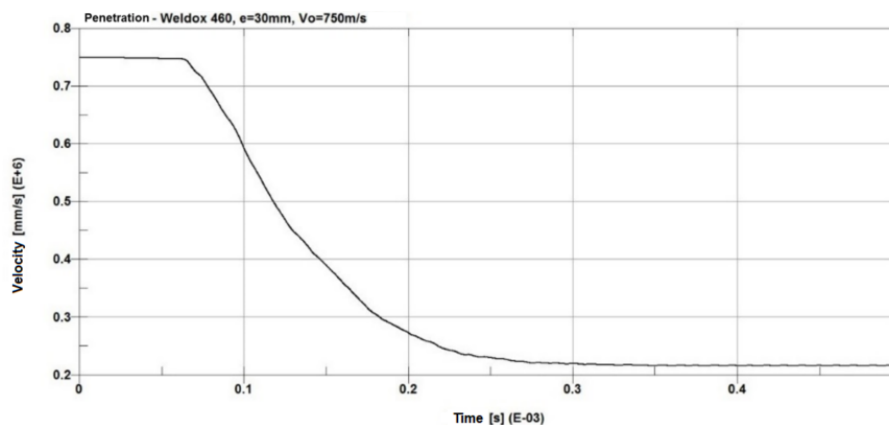


Figure 14 – Projectile speed as a function of time – case 1
 Рис. 14 – Скорость снаряда как функция времени – случай 1
 Слика 14 – Брзина пројектила у функцији времена – случај 1

Figure 15 shows plate displacement as a function of time. It shows that the first movement of the plate occurs after 0.1ms. The maximum plate displacement is 1.4mm.

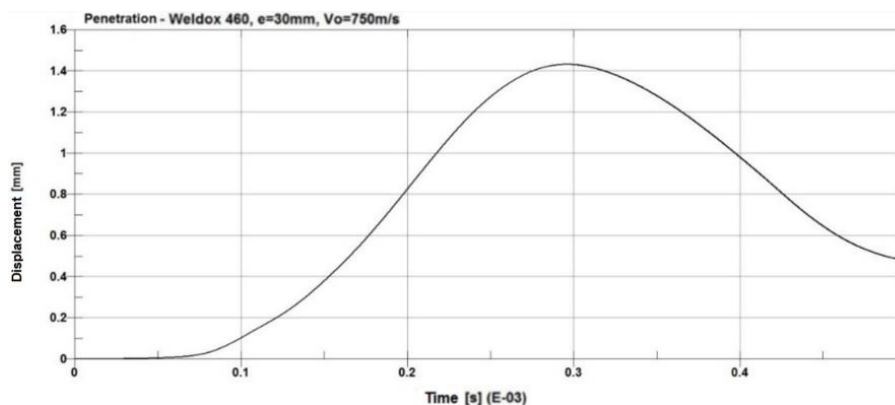


Figure 15 – Plate displacement as a function of time – case 1
 Рис. 15 – Смещение пластины как функция времени – случай 1
 Слика 15 – Померање плоче у функцији времена – случај 1

Case 2 – Plate thickness of 40mm

Figures 16-21 show the Von Misses equivalent stress and penetration effect for armor plate Weldox 460 with a thickness of 40mm.

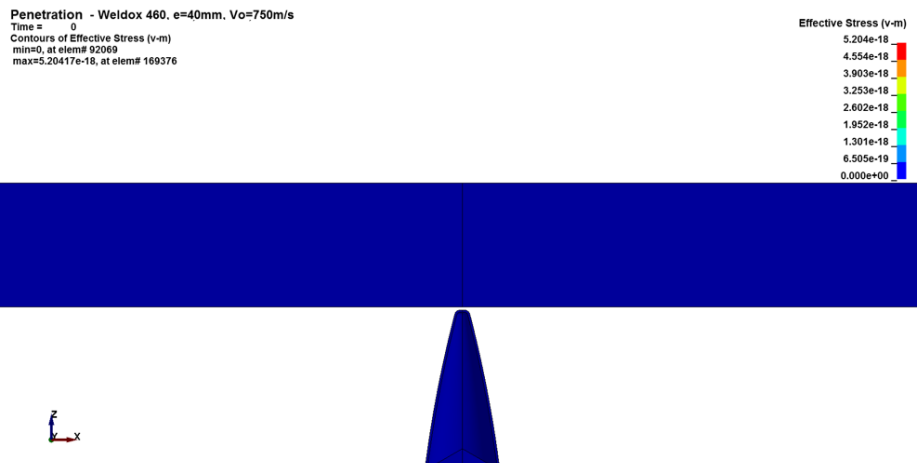


Figure 16 – Von Misses equivalent stress, step 1 – case 2
 Рис. 16 – Эквивалентное напряжение Фон Мизиса, шаг 1 – случай 2
 Слика 16 – Вон Мисесов еквивалентни напон, корак 1 – случај 2

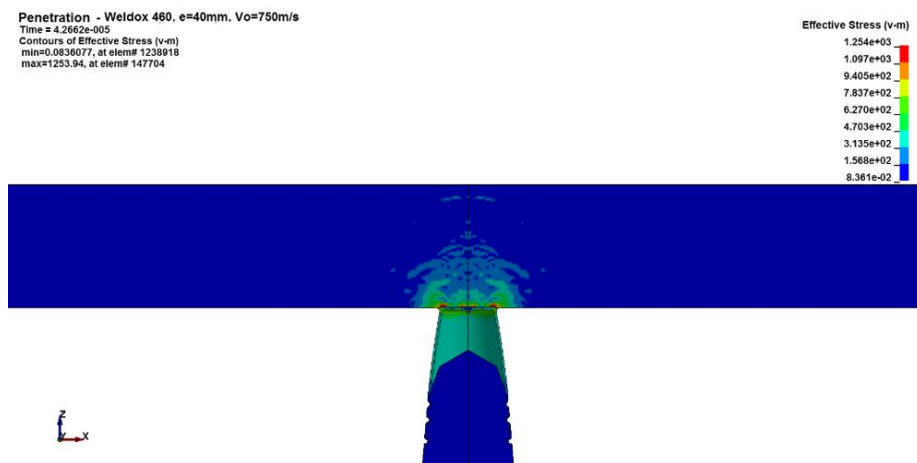


Figure 17 – Von Misses equivalent stress, step 2 – case 2
 Рис. 17 – Эквивалентное напряжение Фон Мизиса, шаг 2 – случай 2
 Слика 17 – Вон Мисесов еквивалентни напон, корак 2 – случај 2

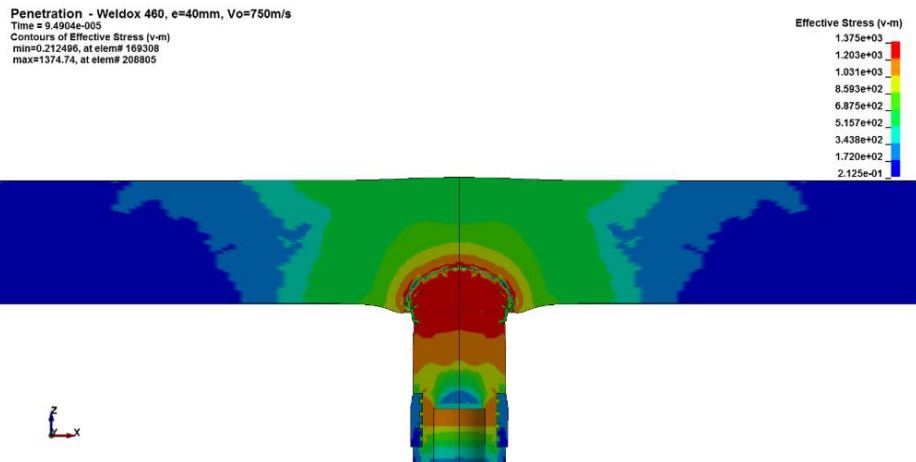


Figure 18 – Von Misses equivalent stress, step 3 – case 2
 Рис. 18 – Эквивалентное напряжение Фон Мизиса, шаг 3 – случай 2
 Слика 18 – Вон Мисесов еквивалентни напон, корак 3 – случај 2

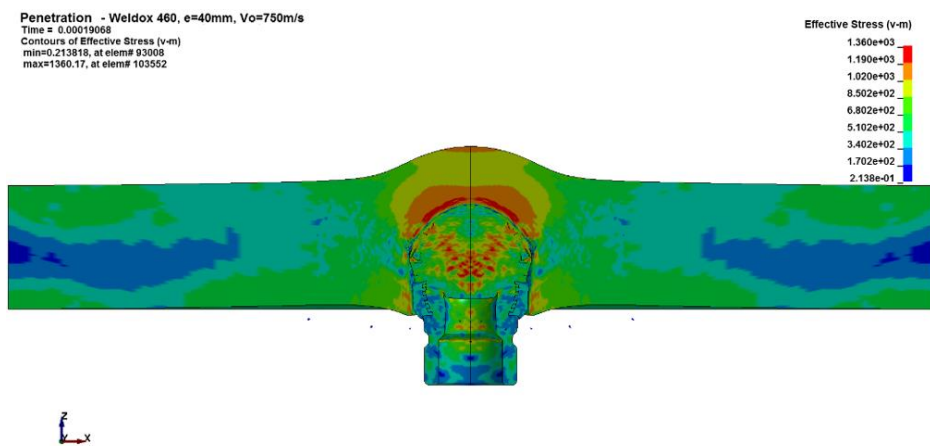


Figure 19 – Von Misses equivalent stress, step 4 – case 2
 Рис. 19 – Эквивалентное напряжение Фон Мизиса, шаг 4 – случай 2
 Слика 19 – Вон Мисесов еквивалентни напон, корак 4 – случај 2

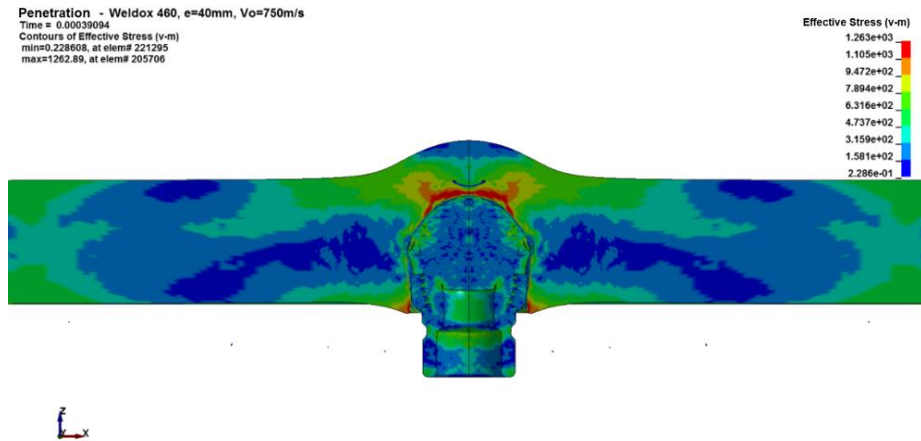


Figure 20 – Von Misses equivalent stress, step 5 – case 2
 Рис. 20 – Эквивалентное напряжение Фон Мизиса, шаг 5 – случай 2
 Слика 20 – Вон Мисесов еквивалентни напон, корак 5 – случај 2

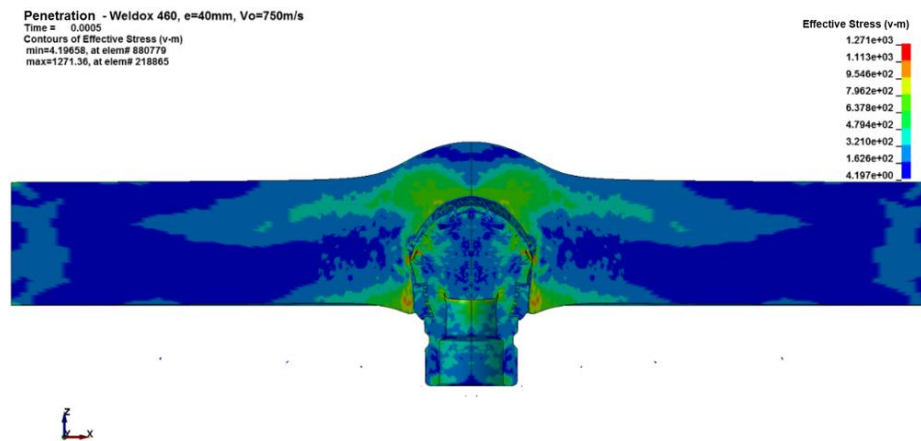


Figure 21 – Von Misses equivalent stress, step 6 – case 2
 Рис. 21 – Эквивалентное напряжение Фон Мизиса, шаг 6 – случай 2
 Слика 21 – Вон Мисесов еквивалентни напон, корак 6 – случај 2

As the results from Figures 16-21 show, the projectile does not have sufficient kinetic energy to achieve a penetration effect in the plate of a thickness of 40mm. After collision, the projectile jams into the plate.

Figure 22 shows the projectile velocity from the moment when it starts penetration into the plate until the moment when it jams into the plate after 0.24ms.

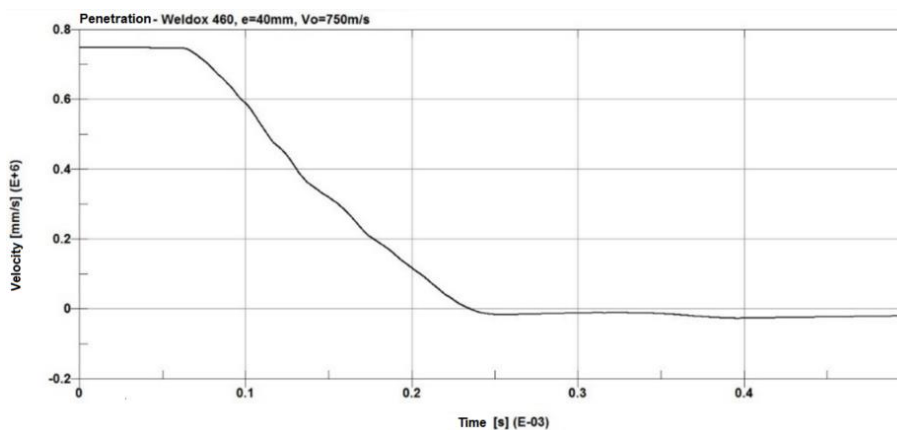


Figure 22 – Projectile speed as a function of time – case 2
 Рис. 22 – Скорость снаряда как функция времени – случай 2
 Слика 22 – Брзина пројектила у функцији времена – случај 2

Figure 23 shows plate displacement as a function of time. It shows that the first movement of the plate occurs after 0.1ms. The maximum plate displacement is 1mm. It is lower than in case 1 because the plate thickness in case 2 is higher.

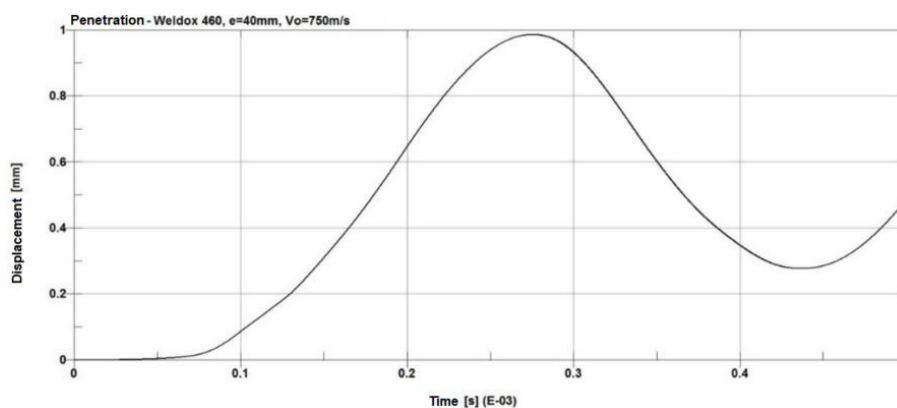


Figure 23 – Plate displacement as a function of time – case 2
 Рис. 23 – Смещение пластины как функция времени – случай 2
 Слика 23 – Померање плоче у функцији времена – случај 2

Additional cases

After numerical simulation and result analysis, the conclusion is that a 30mm armor-piercing projectile at an impact speed of 750m/s achieves the full penetration effect on 30mm thick plates while in the case of a 40mm thickness, it jams into the plate.

For different purposes, it is of great importance to determine the limit (maximum) plate thickness for which the projectile with defined ballistic and material characteristics is able to achieve the full penetration effect.

For the additional simulation cases, the same input parameters are used for the projectile, and the only difference is the armor plate thickness.

Additional numerical simulations are carried out in accordance with the previously defined models using the same initial and boundary conditions. It is found that the full penetration effect is achieved on plates with a thickness of up to 33mm, and after increasing the thickness to higher values, a limited penetration effect then occurs.

Case 3 – Plate thickness of 33mm

Figures 24-29 show the Von Misses equivalent stress and penetration effect for armor plate Weldox 460 with a thickness of 33mm.

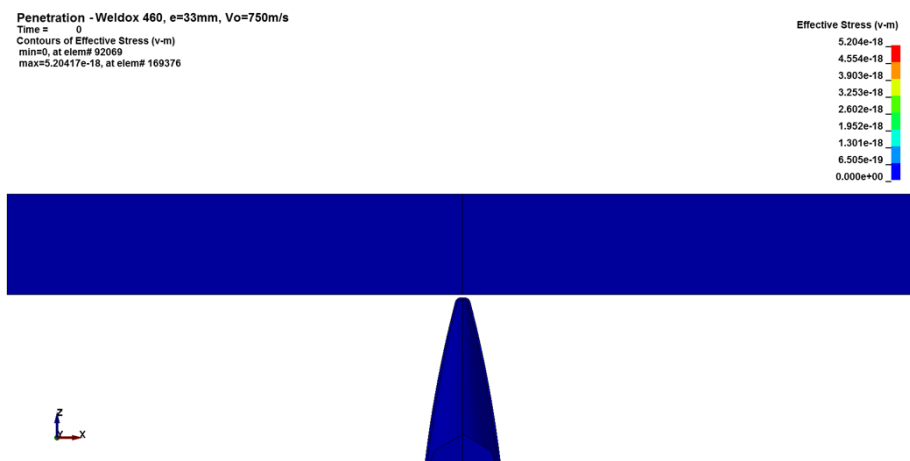


Figure 24 – Von Misses equivalent stress, step 1 – case 3
 Рис. 24 – Эквивалентное напряжение Фон Мизиса, шаг 1 – случай 3
 Слика 24 – Вон Мисесов еквивалентни напон, корак 1 – случај 3

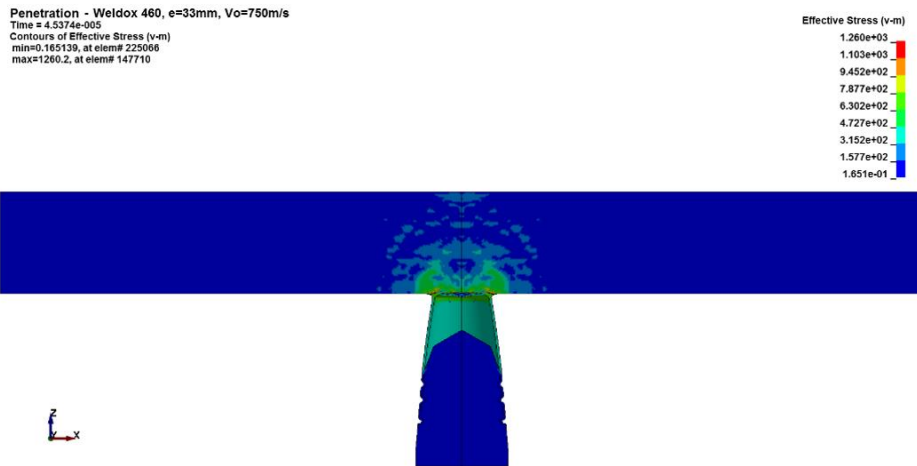


Figure 25 – Von Misses equivalent stress, step 2 – case 3
 Рис. 25 – Эквивалентное напряжение Фон Мизиса, шаг 2 – случай 3
 Слика 25 – Вон Мисесов еквивалентни напон, корак 2 – случај 3

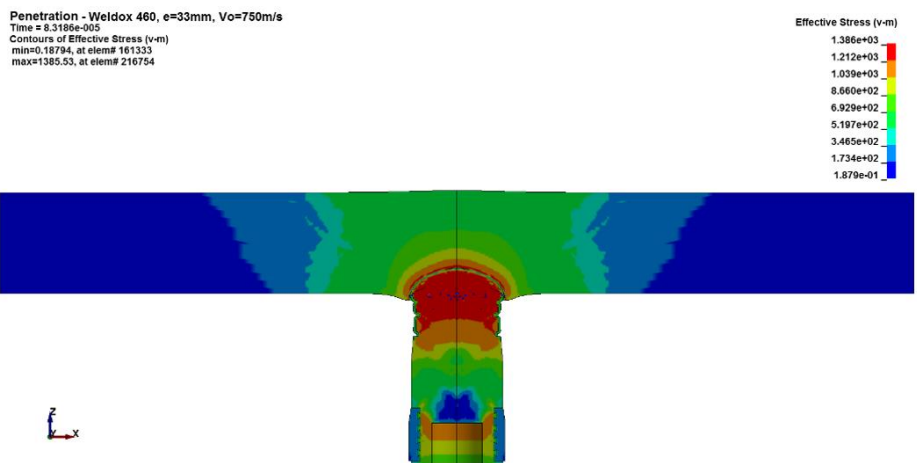


Figure 26 – Von Misses equivalent stress, step 3 – case 3
 Рис. 26 – Эквивалентное напряжение Фон Мизиса, шаг 3 – случай 3
 Слика 26 – Вон Мисесов еквивалентни напон, корак 3 – случај 3

Penetration - Weldox 460, e=33mm, Vo=750m/s
Time = 0.00016722
Contours of Effective Stress (v-m)
min=0.220455, at elem# 161315
max=1383.19, at elem# 197325

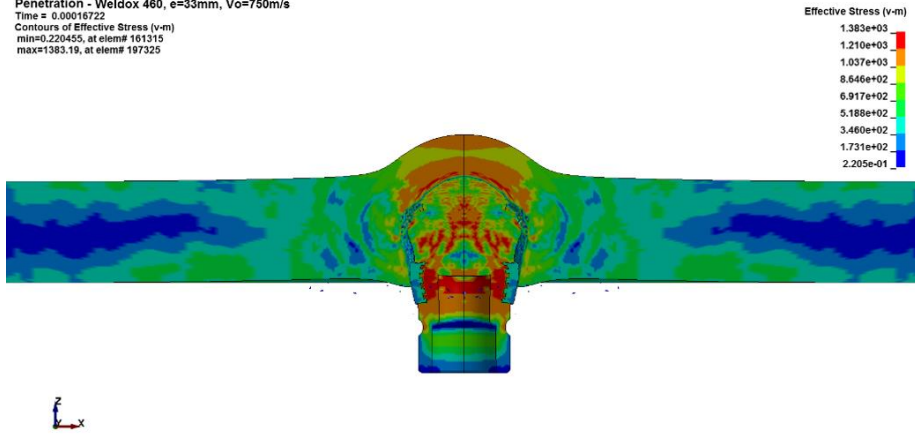


Figure 27 – Von Mises equivalent stress, step 4 – case 3
Рис. 27 – Эквивалентное напряжение Фон Мизиса, шаг 4 – случай 3
Слика 27 – Вон Мисесов еквивалентни напон, корак 4 – случај 3

Penetration - Weldox 460, e=33mm, Vo=750m/s
Time = 0.00031007
Contours of Effective Stress (v-m)
min=6.50263, at elem# 1985518
max=1350.79, at elem# 203691

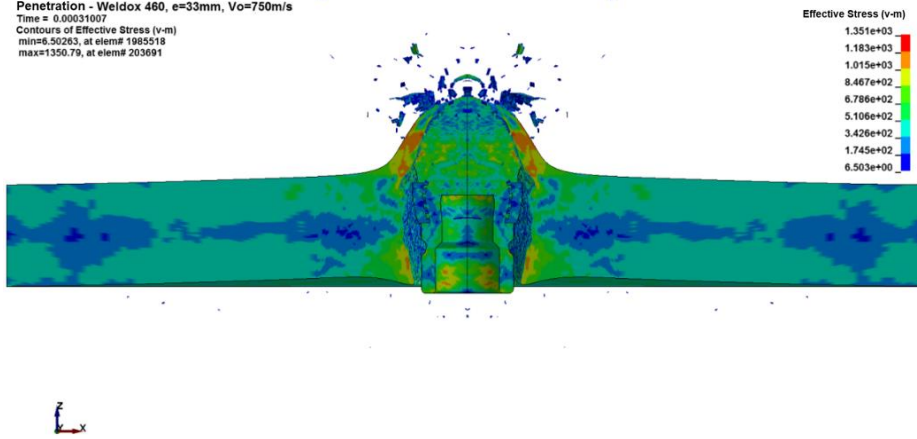


Figure 28 – Von Mises equivalent stress, step 5 – case 3
Рис. 28 – Эквивалентное напряжение Фон Мизиса, шаг 5 – случай 3
Слика 28 – Вон Мисесов еквивалентни напон, корак 5 – случај 3

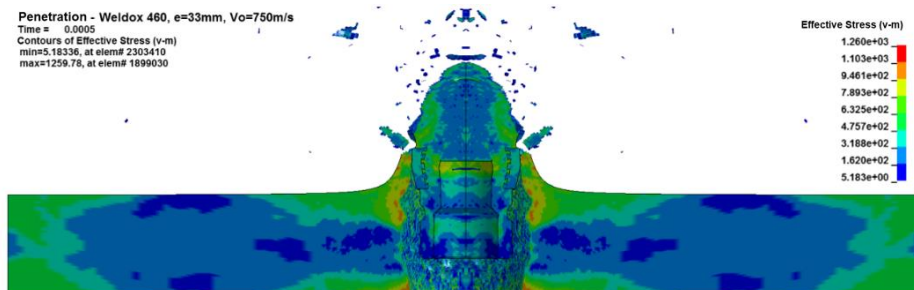


Figure 29 – Von Misses equivalent stress, step 6 – case 3
 Рис. 29 – Эквивалентное напряжение Фон Мизиса, шаг 6 – случай 3
 Слика 29 – Вон Мисесов еквивалентни напон, корак 6 – случај 3

As the results from Figures 24-29 show, the projectile has sufficient kinetic energy to achieve the full penetration effect in the plate of a thickness of 33mm. A large number of fragments are created behind the armor plate as separated parts of both the projectile and the plate.

Figure 30 shows the projectile velocity from the moment when it starts penetration into the plate until the moment of passing through the plate. The projectile velocity after penetration is 70m/s.

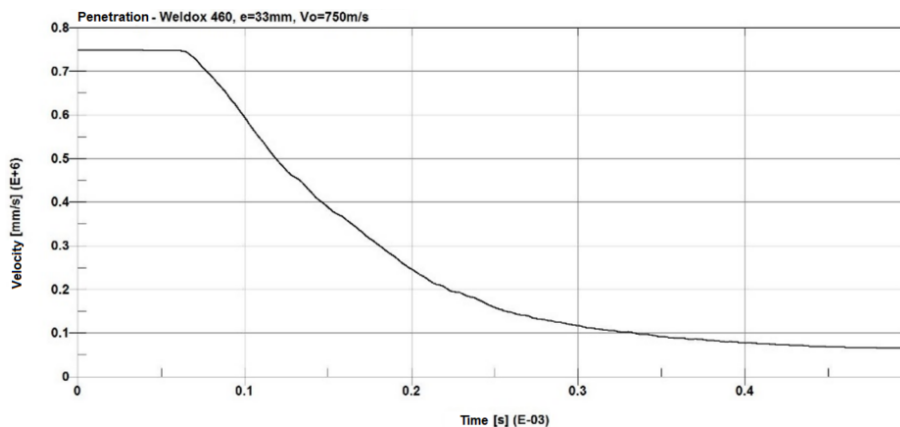


Figure 30 – Projectile speed as a function of time – case 3
 Рис. 30 – Скорость снаряда как функция времени – случай 3
 Слика 30 – Брзина пројектила у функцији времена – случај 3

Figure 31 shows plate displacement as a function of time. It shows that the first movement of the plate occurs after 0.1ms. The maximum plate displacement is 1.2mm.

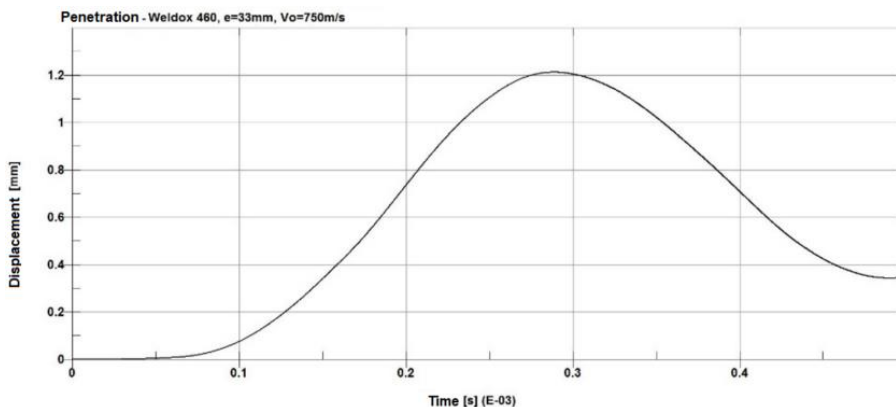


Figure 31 – Plate displacement as a function of time – case 3
 Рис. 31 – Смещение пластины как функция времени – случай 3
 Слика 31 – Померање плоче у функцији времена – случај 3

Case 4 – Plate thickness of 34mm

Figures 32-37 show the Von Misses equivalent stress and penetration effect for armor plate Weldox 460 with a thickness of 34mm.

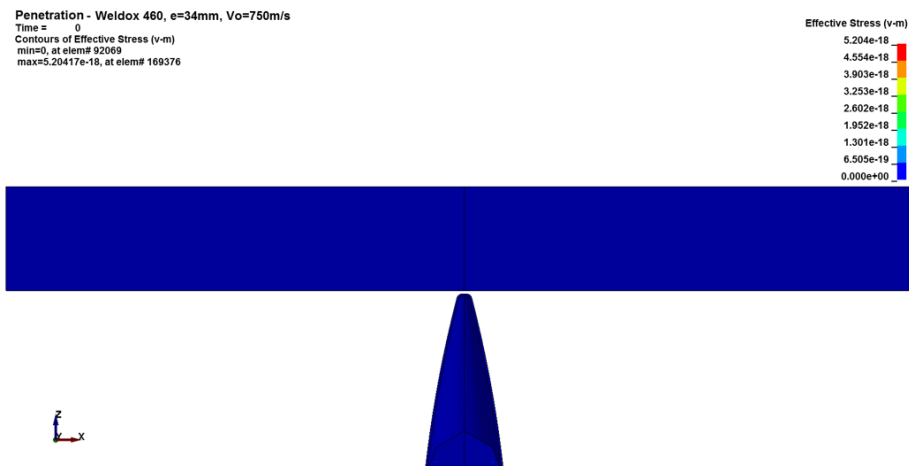


Figure 32 – Von Misses equivalent stress, step 1 – case 4
 Рис. 32 – Эквивалентное напряжение Фон Мизиса, шаг 1 – дело 4
 Слика 32 – Вон Мисесов еквивалентни напон, корак 1 – случај 4

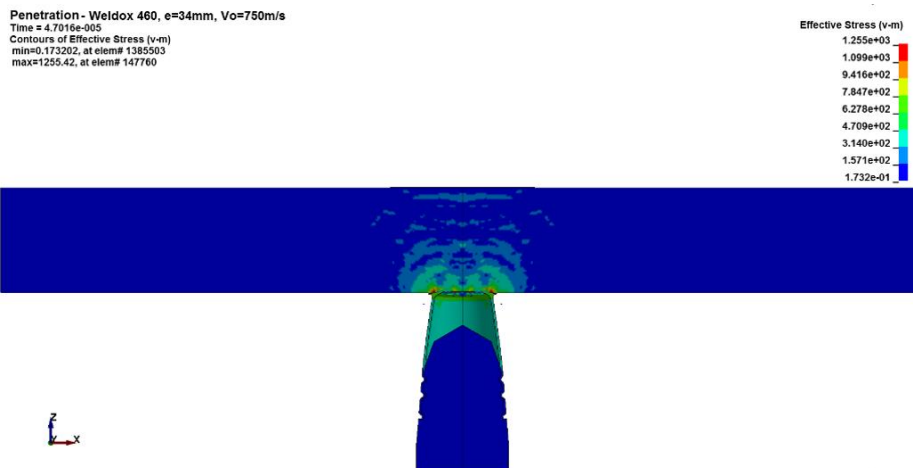


Figure 33 – Von Mises equivalent stress, step 2 – case 4
 Рис. 33 – Эквивалентное напряжение Фон Мизиса, шаг 2 – случай 4
 Слика 33 – Вон Мисесов еквивалентни напон, корак 2 – случај 4

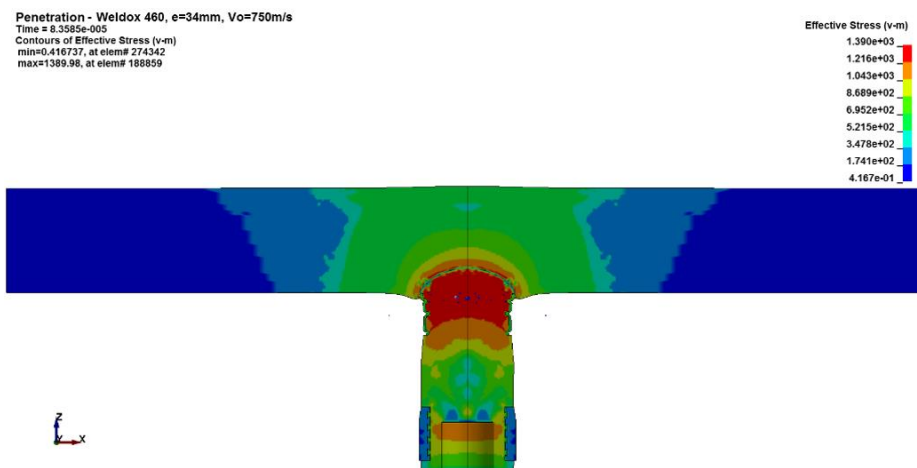


Figure 34 – Von Mises equivalent stress, step 3 – case 4
 Рис. 34 – Эквивалентное напряжение Фон Мизиса, шаг 3 – случай 4
 Слика 34 – Вон Мисесов еквивалентни напон, корак 3 – случај 4

Penetration - Weldox 460, e=34mm, Vo=750m/s
Time = 0.00012538
Contours of Effective Stress (v-m)
min=0.214252, at elem# 92811
max=1380.58, at elem# 204841

Effective Stress (v-m)
1.381e+03
1.208e+03
1.035e+03
8.629e+02
6.904e+02
5.179e+02
3.453e+02
1.728e+02
2.143e-01

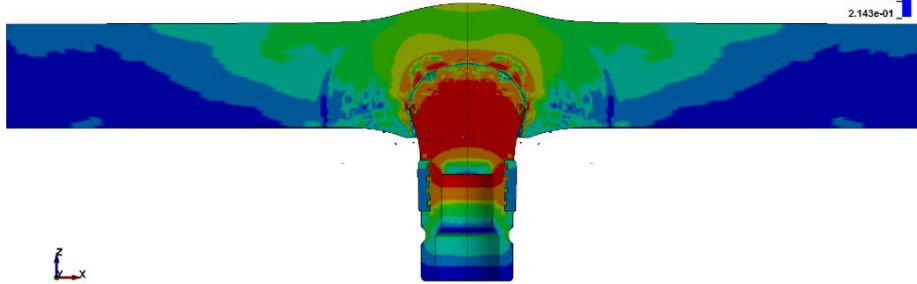


Figure 35 – Von Mises equivalent stress, step 4 – case 4
Рис. 35 – Эквивалентное напряжение Фон Мизиса, шаг 4 – случай 4
Слика 35 – Вон Мисесов еквивалентни напон, корак 4 – случај 4

Penetration - Weldox 460, e=34mm, Vo=750m/s
Time = 0.00020113
Contours of Effective Stress (v-m)
min=0.189891, at elem# 213323
max=1365.63, at elem# 245785

Effective Stress (v-m)
1.366e+03
1.195e+03
1.024e+03
8.536e+02
6.829e+02
5.122e+02
3.415e+02
1.709e+02
1.889e-01

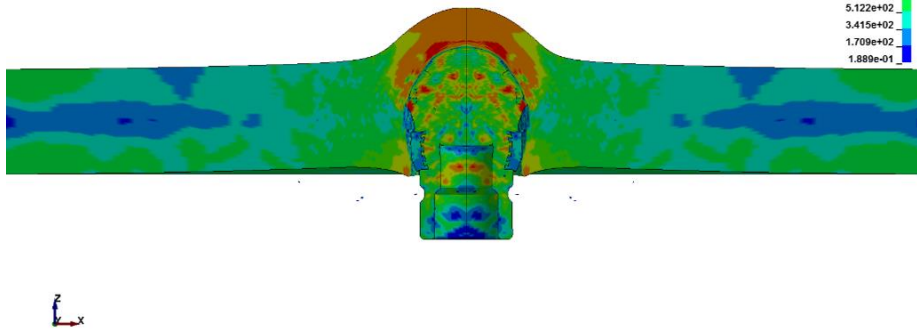


Figure 36 – Von Mises equivalent stress, step 5 – case 4
Рис. 36 – Эквивалентное напряжение Фон Мизиса, шаг 5 – случай 4
Слика 36 – Вон Мисесов еквивалентни напон, корак 5 – случај 4

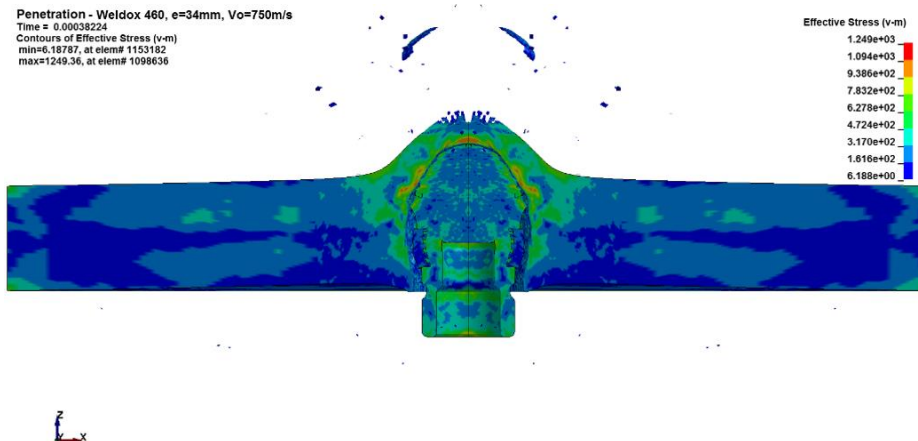


Figure 37 – Von Mises equivalent stress, step 6 – case 4
 Рис. 37 – Эквивалентное напряжение Фон Мизиса, шаг 6 – случай 4
 Слика 37 – Вон Мисесов еквивалентни напон, корак 6 – случај 4

As the results from Figures 32-37 show, the projectile does not have sufficient kinetic energy to achieve the penetration effect in the plate of a thickness of 34mm. After collision with the plate, the projectile jams into the plate. But, differently from case 2 with the 40mm plate, in this case projectile's semi penetration creates a number of fragments, which can also have a big impact on potential targets behind the plate. Figure 38 shows the projectile velocity from the moment when it starts penetration into the plate until the moment when it jams into the plate after 0.3ms.

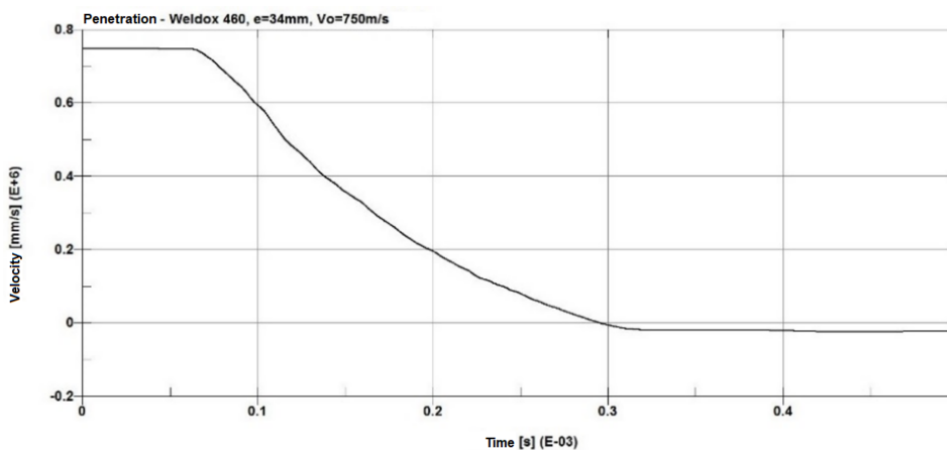


Figure 38 – Projectile speed as a function of time – case 4
 Рис. 38 – Скорость снаряда как функция времени – случай 4
 Слика 38 – Брзина пројектила у функцији времена – случај 4

Figure 39 shows plate displacement as a function of time. It shows that the first movement of the plate occurs after 0.1ms. The maximum plate displacement is 1.4mm.

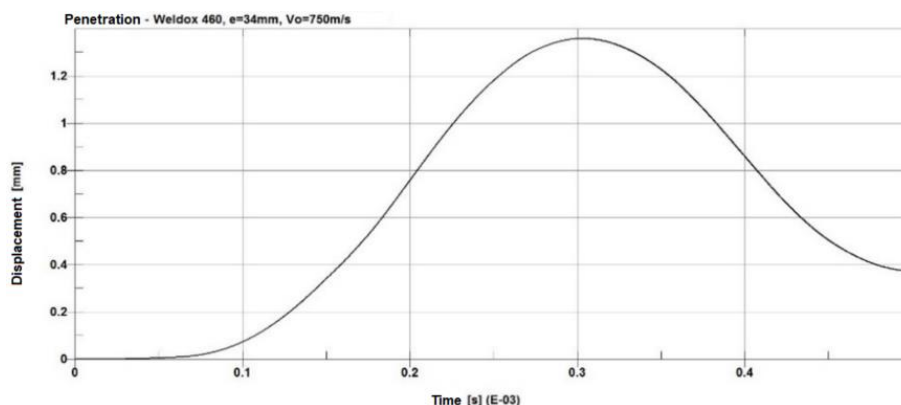


Figure 39 – Plate displacement as a function of time – case 4
 Рис. 39 – Смещение пластины как функция времени – случай 4
 Слика 39 – Померање плоче у функцији времена – случај 4

Conclusion

Armor-piercing projectiles are designed to penetrate either body armor or vehicle armor. Due to their high kinetic energy at the time of impact with an obstacle and their body's exceptional endurance, they are able to penetrate armor.

It is extremely difficult to represent the impact of an armor-piercing projectile, but the models created successfully describe the real issue of projectile penetration (or with a certain deviation). In recent times, analysis using the finite element method has proven to be one of effective approaches to solving such and similar problems.

In this paper, a numerical simulation of the penetration process of a 30mm anti-aircraft armor projectile into Weldox 460 alloy plates of different thicknesses was performed. Spasić (2018) has also taken into account the analysis of Weldox 460 armor steel during numerical modeling of a projectile impact on metal structures and shown its behavior when it is in collision with projectiles of different shapes.

Based on a detailed review of the literature, it is found that deformation, strain rate, temperature, and pressure are the key factors that have the greatest influence on the penetration process.

In order to correctly describe these phenomena, it is necessary to define equations of state and models of material behavior. The Johnson–

Cook material model and the Mie–Grüneisen equation of state were used to define the models.

To determine the maximum penetrating ability of the projectile, four simulation cases with different plate thicknesses were performed.

In case 1, with a plate thickness of 30mm, and case 3, with a plate thickness of 33mm, the projectile had the full penetration effect into the defined plates, because the projectile's impact velocity and kinetic energy were higher than needed for the full penetration effect. The projectile velocity behind the plate in case 1 is 220m/s, and in case 3 the velocity is 70m/s.

In case 2, the projectile jammed into the plate with a thickness of 40mm, while in case 4, the projectile jammed into the plate with a thickness of 34mm, but its semi-penetration generated a larger number of fragments behind the plate. In all four cases, the first plate displacements occur after 0.1ms of the analysis.

The projectile with the defined ballistic material and characteristics has the ability to fully penetrate the W尔多x 460 plate with a maximum thickness of 33mm.

The calculated ballistic armor steel plate thickness of 33mm is not produced as a standard monobloc plate, but in reality, this thickness can be achieved as a sandwich armor plate with one thicker (e.g., 30mm) and one thinner plate (e.g., 3mm), or with one 30mm plate placed at some angle to the vertical axis.

When defining the ballistic protection of an armored vehicle against projectiles of defined characteristics, it is necessary to use armor steel with a thickness greater than the calculated one in order to neutralize a potential effect of separate fragments from the other side of the plate.

Despite the fact that analytical and numerical methods of calculation can provide correct data about the character of certain phenomena, it is always desirable and necessary, first of all, to carry out experimental tests on the training ground and, after obtaining certain results, to make the necessary corrections and examine the given phenomenon with numerical methods in order to solve the problem more easily and economically.

References

Bataev, I.A., Tanaka, S., Zhou, Q., Lazurenko, D.V., Jorge Junior, A.M., Bataev, A.A., Hokamoto, K., Mori, A. & Chen, P. 2019. Towards better understanding of explosive welding by combination of numerical simulation and experimental study. *Materials & Design*, 169, art.number:107649. Available at: <https://doi.org/10.1016/j.matdes.2019.107649>.

Champagne, V.K., Helfritsch, D.J., Trexler, M.D. & Gabriel, B.M. 2010. The effect of cold spray impact velocity on deposit hardness. *Modelling and Simulation in Materials Science and Engineering*, 18, art.number:065011. Available at: <https://doi.org/10.1088/0965-0393/18/6/065011>.

Elek, P. 2018. *Balistika na cilju*. Belgrade: University of Belgrade, Faculty of Mechanical Engineering (in Serbian). ISBN: 978-86-7083-966-3 [online]. Available at: https://www.mas.bg.ac.rs/_media/biblioteka/izdanja/17/17.02.pdf [Accessed: 03 March 2023].

Heuzé, O. 2012. General form of the Mie–Grüneisen equation of state. *Comptes Rendus Mécanique*, 340(10), pp.679-687. Available at: <https://doi.org/10.1016/j.crme.2012.10.044>.

Liu, Z.S., Swaddiwudhipong, S. & Islam, M.J. 2012. Perforation of steel and aluminum targets using a modified Johnson–Cook material model. *Nuclear Engineering and Design*, 250, pp.108-115. Available at: <https://doi.org/10.1016/j.nucengdes.2012.06.026>.

Murthy, V.C.A.D. & Santhanakrishnanan, S. 2020. Isogrid lattice structure for armouring applications. *Procedia Manufacturing*, 48, pp.e1-e11. Available at: <https://doi.org/10.1016/j.promfg.2020.05.099>.

Rezasefat, M., Mostofi, T.M., Babaei, H., Ziya-Shamami, M. & Alitavoli, M. 2018. Dynamic plastic response of double-layered circular metallic plates due to localized impulsive loading. *Proceedings of the Institution of Mechanical Engineers, Part L: Journal of Materials: Design and Applications*, 233(7), pp.1449-1471. Available at: <https://doi.org/10.1177/1464420718760640>.

Spasić, D.M. 2018. Numerical modeling of the impact of projectiles on metal structures. *Vojnotehnički glasnik/Military Technical Courier*, 66(1), pp.63-105. Available at: <https://doi.org/10.5937/vojtehg66-9604>.

Wang, X. & Shi, J. 2013. Validation of Johnson-Cook plasticity and damage model using impact experiment. *International Journal of Impact Engineering*, 60, pp.67-75. Available at: <https://doi.org/10.1016/j.ijimpeng.2013.04.010>.

Wilkins, M.L. 1999. *Computer Simulation of Dynamic Phenomena*. Heidelberg: Springer Berlin. Available at: <https://doi.org/10.1007/978-3-662-03885-7>.

Численный анализ процесса проникновения бронебойного снаряда калибра 30-мм

Предраг Р. Пантович^а, **коресподент**, Мирослав М. Живкович^а, Владимир П. Милованович^а, Ненад М. Милорадович^б

^а Крагуевацкий университет, факультет инженерных наук, г. Крагуевац, Республика Сербия

^б Министерство обороны Республики Сербия, г. Белград, Республика Сербия

РУБРИКА ГРНТИ: 78.25.00 Вооружение и военная техника
ВИД СТАТЬИ: оригинальная научная статья

Резюме:

Введение/цель: Тонкие пластины из высокопрочной стали часто используются как в гражданских, так и в военных системах баллистической защиты. При выборе вида сплава, который будет использоваться, необходимо соблюдать ряд критериев, таких как: условия использования, соответствующие баллистические характеристики, вес, размеры и стоимость. В данной статье проведен численный анализ проникновения бронебойного снаряда калибра 30 мм со скоростью 750 м/с с расстояния 1000 м в пластины различной толщины из легированной стали Weldox 460.

Методы: Анализ был выполнен с использованием численных методов и моделирования методом конечных элементов для расчета напряжений и деформаций, вызванных вследствие проникновения. Для определения характеристик материала использовались физическая модель Джонсона-Кука и модель разрушения материалов. В данной статье для утверждения моделей и выполнения численных расчетов использовались программные пакеты FEMAP и LS Dyna.

Результаты: Для определения результатов проведенного численного анализа использовались значения напряжений и деформаций. Представлены также результаты по четырем различным толщинам броневых листов: 30мм, 33мм, 34мм и 40мм. Результаты показывают эффект проникновения и взаимодействие между снарядом и бронепластиной.

Выводы: Моделирование воздействия бронебойных преград очень сложное, объемное и требовательное, а сформированные модели очень удачно (или с некоторым отклонением) аппроксимируют реальную задачу проникновения снаряда. В последнее время анализ с использованием метода конечных элементов является одним из наиболее эффективных подходов к решению подобных задач. Наибольшее влияние на бронепробиваемость снаряда оказывают материал и размеры преграды, а также баллистические параметры снаряда и материалы изготовления. При сохранении всех входных параметров на одном уровне и увеличении толщины мишени увеличивается ее сопротивление к проникновению.

Ключевые слова: броня, снаряд, проникновение, Weldox 460, численные методы.

Нумеричка анализа процеса пенетрације панцирног пројектила 30 mm

Предраг Р. Пантовић^а, аутор за преписку, Мирослав М. Живковић^а,
Владимир П. Миловановић^а, Ненад М. Милорадовић^б

^а Универзитет у Крагујевцу, Факултет инжењерских наука,
Крагујевац, Република Србија

^б Министарство одбране Републике Србије, Београд, Република Србија

ОБЛАСТ: машинско инжењерство, материјали
КАТЕГОРИЈА (ТИП) ЧЛАНКА: оригинални научни рад

Сажетак:

Увод/циљ: Танке плоче од челика високе чврстоће често се користе у цивилним и војним системима балистичке заштите. За одабир врсте легуре која ће се користити потребно је испунити низ критеријума, као што су услови употребе, жељене балистичке перформансе, тежина, димензије и цена. У раду је урађена нумеричка анализа пробојности панцирно-пробојног пројектила калибра 30 mm, брзине 750 m/s, на удаљености од 1000 m, у плоче различите дебљине од легуре челика Weldox 460.

Метод: Анализа је извршена нумеричким методама и моделирањем коначних елемената за прорачун напона и деформација узрокованих ефектом пробојности. За дефинисање карактеристика материјала коришћен је Џонсон-Куков материјални модел и модел лома материјала, а за дефинисање модела и извођење нумеричког прорачуна коришћени су софтверски пакети FEMAP и LS Dyna.

Резултати: За дефинисање резултата извршене нумеричке анализе коришћене су вредности напона и деформација. Приказани су резултати за четири различите дебљине оклопних плоча: 30 mm, 33 mm, 34 mm и 40 mm. Показан је ефекат пенетрације и интеракција између пројектила и оклопне плоче.

Закључак: Моделовање утицаја оклопних препрека је веома сложено, обимно и захтевно, а формирану модели на веома успешан начин (или са одређеним одступањем) апроксимирају стварни проблем продора пројектила. Анализа методом коначних елемената се, у новије време, показала као један од ефикаснијих приступа за решавање оваквих и сличних проблема. Материјал и димензије препреке, као и материјални и балистички параметри пројектила, имају највећи утицај на продор пројектила. Одржавањем свих улазних параметара на истом нивоу, и повећањем дебљине мете, повећава се и њен отпор на продор.

Кључне речи: оклоп, пројектил, продор, Weldox 460, нумеричке методе.

Paper received on / Дата получения работы / Датум пријема чланка: 04.04.2023.
Manuscript corrections submitted on / Дата получения исправленной версии работы /
Датум достављања исправки рукописа: 14.06.2023.

Paper accepted for publishing on / Дата окончательного согласования работы / Датум
коначног прихватања чланка за објављивање: 16.06.2023.

© 2023 The Authors. Published by Vojnotehnički glasnik / Military Technical Courier
(www.vtg.mod.gov.rs, втг.мо.упр.срб). This article is an open access article distributed under the
terms and conditions of the Creative Commons Attribution license
(<http://creativecommons.org/licenses/by/3.0/rs/>).

© 2023 Авторы. Опубликовано в «Военно-технический вестник / Vojnotehnički glasnik / Military
Technical Courier» (www.vtg.mod.gov.rs, втг.мо.упр.срб). Данная статья в открытом доступе и
распространяется в соответствии с лицензией «Creative Commons»
(<http://creativecommons.org/licenses/by/3.0/rs/>).

© 2023 Аутори. Објавио Војнотехнички гласник / Vojnotehnički glasnik / Military Technical Courier
(www.vtg.mod.gov.rs, втг.мо.упр.срб). Ово је чланак отвореног приступа и дистрибуира се у
складу са Creative Commons лиценцом (<http://creativecommons.org/licenses/by/3.0/rs/>).

